

Tribenzylidenemethane complexes of ruthenium. Synthesis and effects of the diastereoisomerism on the crystal packing

Gerhard E. Herberich, Thomas P. Spaniol *

Institut für Anorganische Chemie, Technische Hochschule Aachen, D-52056 Aachen, Germany

Received 16 October 1998

Abstract

Reaction of the tribenzylidenemethane (TBM) dianion with $[\text{RuCl}_2(\text{C}_6\text{H}_6)]_2$ yields a diastereoisomeric mixture of the metal complexes with formula $[\text{Ru}(\text{TBM})(\text{C}_6\text{H}_6)]$, which can be separated by column chromatography and fractional crystallisation. The crystal structures of both compounds were determined by X-ray diffraction on single crystals. The arrangement of the phenyl rings has a major influence on the build-up of the crystal lattice. The molecule containing the propeller-shaped ligand of C_3 symmetry crystallises in a layer structure with a packing arrangement that is caused by the fragment TBM. The close similarity with the crystal structure of $[\text{Ta}(\text{TBM})(\eta^5\text{-C}_5\text{H}_5)(\text{CH}_3)_2]$ shows that the fragment TBM can serve as a synthon for crystal engineering. © 1999 Elsevier Science S.A. All rights reserved.

Keywords: Tribenzylidenemethane; Diastereoisomers; Crystal engineering

1. Introduction

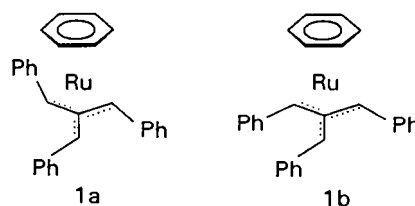
Trimethylenemethane $\text{C}(\text{CH}_2)_3$ (TMM) is a versatile ligand to transition metals [1]. The synthesis of its complexes occasionally uses the dianion TMM^{2-} as a ligand source [2–5]. In analogy, the related dianion of tribenzylidenemethane $[\text{Li}(\text{TMEDA})]_2[\text{C}(\text{CHPh})_3]$ [6,7] can be used to introduce the ligand TBM [5,8,9]. Transition metal complexes containing this ligand were used as catalysts for the polymerisation of olefins [5,8,9]. The free dianion of TBM is prochiral, but its transition metal complexes will be chiral. In this paper we show that the reaction with TBM^{2-} gives the two diastereomeric isomers of $(\eta^6\text{-benzene})(\eta^4\text{-tribenzylidenemethane})\text{ruthenium}$. Here, we also describe the crystal structures of both compounds with emphasis on the individual packing arrangements.

* Corresponding author. Present address: Institut für Anorganische Chemie und Analytische Chemie, Johannes Gutenberg-Universität Mainz, D-55099 Mainz, Germany. Tel.: +49-6131-393918; fax: +49-6131-395605.

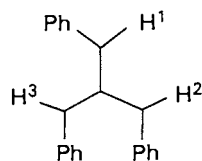
E-mail address: spaniol@mail.uni-mainz.de (T.P. Spaniol)

2. Synthesis and spectroscopic characterisation

Treatment of $[\text{RuCl}_2(\text{C}_6\text{H}_6)]_2$ with $[\text{Li}(\text{TMEDA})]_2[\text{C}(\text{CHPh})_3]$ in tetrahydrofuran solution gives a mixture of the two isomers **1a** and **1b** in moderate yield. In the lithium dianion, the benzylidene groups are configurationally mobile and the NMR data in solution show only the propeller-like dianion of C_3 symmetry which is also observed in the crystalline state [7]. In contrast to this situation, the tribenzylidenemethane ligands are configurationally fixed in the ruthenium complexes. The observed product ratio of 3:1 reflects kinetic control during product formation.



The two diastereoisomers can easily be separated by fractional crystallisation. Both compounds are yellow crystalline solids and can be described as derivatives of the complex $[\text{Ru}(\text{TMM})(\text{C}_6\text{H}_6)]$ **2** [4]. The symmetries of the isomers **1a** and **1b** are reflected in the NMR spectra. The chemical equivalence of the benzylidene groups in **1a** is lost in **1b**. In the ^1H -NMR spectra one resonance is seen for the TMM protons in **1a** whereas in **1b** three resonances are found. The good resolution allows a closer assignment via the coupling constants. It has early been noted that within various $^4J_{\text{HH}}$ couplings only the *w*-coupling can easily be detected [10]. In agreement with this notion one of the TMM protons of **1b** is seen as a singlet resonance (3.15 ppm for H^1) while the remaining two protons H^2 and H^3 at 3.32 and 4.41 ppm appear as an AB system with $^4J = 1.5$ Hz.



We assign the low field resonance to H^3 as this proton has a similar environment as the TMM protons in **1a** (4.18 ppm). A recent report describes a TBM metal complex with the analogous unsymmetrical arrangement of the phenyl rings [9]. In that work, the ligand was built up in the coordination sphere of the metal centre. However, for all other transition metal complexes that were obtained from the dianion of TBM, only compounds with the symmetrical propeller-shaped ligand were found [5,8,9].

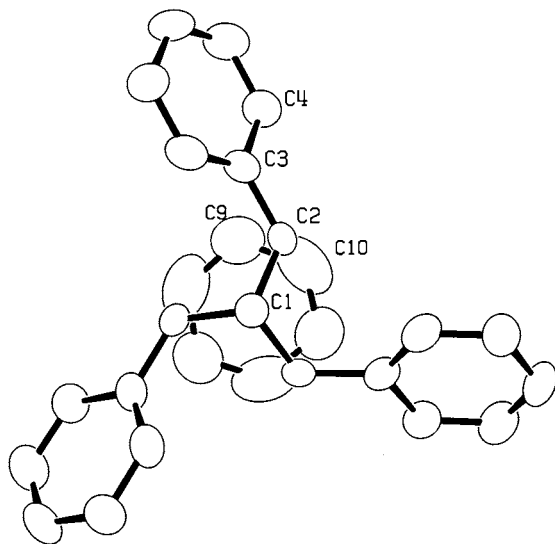


Fig. 1. ORTEP plot (30% probability ellipsoids) of **1a** (showing only one of the crystallographically independent molecules).

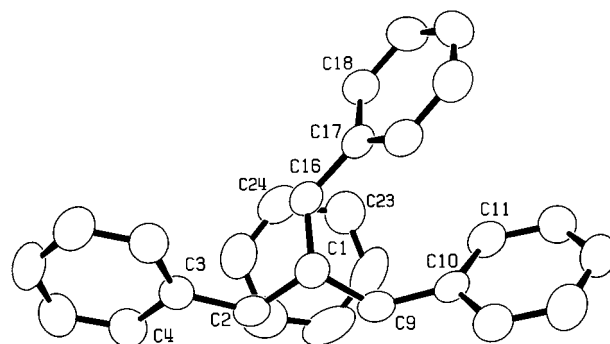


Fig. 2. ORTEP plot (30% probability ellipsoids) of **1b**.

3. Molecular structures

The structures of both diastereoisomers **1a** and **1b** have been determined by X-ray diffraction on single crystals (Figs. 1 and 2, Tables 1–5); **1a** is found with two crystallographically independent molecules in the unit cell.

Their molecular structures closely resemble each other and the core structure is very similar to that found in the TMM complex **2** [4]. A comparison between the structures of **1a,b** and **2** shows that the distances between the metal and the C_4 -carbon atoms are equal within experimental accuracy. The phenyl ring substituents do not lead to wider distances. However, for zirconium complexes the distances between the C_4 -fragment of a TMM ligand and the metal were

Table 1
Co-ordinates of non-hydrogen atoms for **1a**

Atom	x	y	z	U_{eq}^a
Ru(1)	0.0000	0.0000	−0.01579(5)	39.7(2)
C(1)	0.0000	0.0000	−0.1436(5)	35(2)
C(2)	0.1043(6)	0.1198(7)	−0.1215(4)	34(1)
C(3)	0.1058(5)	0.2388(5)	−0.1358(3)	39(1)
C(4)	0.1862(6)	0.3419(6)	−0.0867(4)	50(1)
C(5)	0.1914(7)	0.4539(6)	−0.0973(5)	58(2)
C(6)	0.1221(8)	0.4691(8)	−0.1583(5)	54(2)
C(7)	0.042(1)	0.368(1)	−0.2090(5)	54(2)
C(8)	0.0374(6)	0.2560(6)	−0.1970(4)	47(2)
C(9)	0.043(2)	0.126(1)	0.0914(5)	91(4)
C(10)	0.1259(9)	0.085(2)	0.0917(5)	88(3)
Ru(2)	0.6667	0.3333	−0.00007(5)	47.9(2)
C(21)	0.6667	0.3333	0.1278(5)	39(2)
C(22)	0.7901(8)	0.3607(7)	0.1076(4)	44(2)
C(23)	0.9059(5)	0.4763(5)	0.1223(4)	39(1)
C(24)	0.9162(6)	0.5610(6)	0.1841(4)	46(2)
C(25)	1.033(1)	0.6634(7)	0.2027(6)	56(2)
C(26)	1.1344(8)	0.6848(8)	0.1601(6)	61(2)
C(27)	1.1254(6)	0.6039(8)	0.0997(5)	56(2)
C(28)	1.0116(6)	0.4999(7)	0.0804(4)	49(1)
C(29)	0.575(2)	0.365(2)	−0.1071(6)	96(4)
C(30)	0.541(1)	0.245(1)	−0.1083(6)	108(5)

^a The anisotropic thermal parameters are given in the form of their isotropic equivalents (in 10^3 \AA^2).

Table 2
Selected bond distances (Å) and angles (°) for **1a**

Bond length (Å)			
Ru1–C(1)	2.038(8)	Ru2–C(21)	2.040(9)
Ru1–C(2)	2.196(7)	Ru2–C(22)	2.215(8)
Ru1–C(9)	2.20(1)	Ru2–C(29)	2.20(1)
Ru1–C(10)	2.205(7)	Ru2–C(30)	2.22(1)
C(1)–C(2)	1.449(7)	C(21)–C(22)	1.435(9)
C(2)–C(3)	1.490(9)	C(22)–C(23)	1.46(1)
C(9)–C(10)	1.37(2)	C(29)–C(30)	1.33(2)
C(9)–C(10)'	1.41(2)	C(29)–C(30)'	1.45(2)
Bond angles (°)			
C(2)–C(1)–C(2)	114.3(3)	C(22)–C(21)–C(22)	115.1(3)
C(1)–C(2)–C(3)	123.1(5)	C(21)–C(22)–C(23)	127.7(6)
C(2)–C(3)–C(4)	118.2(6)	C(22)–C(23)–C(24)	121.9(6)
C(2)–C(3)–C(8)	124.1(5)	C(22)–C(23)–C(28)	120.1(6)

found to be shorter than the corresponding bond lengths in a related TBM ligand [5]. Both crystallographically independent molecules of **1a** have a nearly identical structure within experimental accuracy (see Table 2). The angles that the phenyl rings form with the *c*-axis deviate only slightly with values of ca. 47 and 49°.

Table 3
Coordinates of non-hydrogen atoms for **1b**

Atom	<i>x</i>	<i>y</i>	<i>z</i>	<i>U</i> _{eq} ^a
Ru	0.15787(3)	0.34867(2)	0.35128(2)	41.3(1)
C(1)	0.0121(3)	0.2878(2)	0.4033(2)	40.7(8)
C(2)	0.1299(3)	0.2648(3)	0.4683(2)	41.8(8)
C(3)	0.1926(3)	0.1673(3)	0.4889(2)	41.7(8)
C(4)	0.3248(3)	0.1623(3)	0.5347(2)	52.0(9)
C(5)	0.3876(4)	0.0746(4)	0.5579(3)	62(1)
C(6)	0.3208(5)	−0.0123(4)	0.5370(3)	65(1)
C(7)	0.1896(4)	−0.0113(3)	0.4927(3)	60(1)
C(8)	0.1265(4)	0.0778(3)	0.4699(2)	51.4(9)
C(9)	−0.0151(3)	0.3936(3)	0.4023(2)	43.5(8)
C(10)	−0.1335(3)	0.4480(2)	0.3514(2)	41.0(8)
C(11)	−0.1566(4)	0.4756(3)	0.2631(2)	55(1)
C(12)	−0.2701(4)	0.5249(3)	0.2218(3)	60(1)
C(13)	−0.3639(4)	0.5486(3)	0.2678(3)	59(1)
C(14)	−0.3422(4)	0.5258(3)	0.3564(3)	61(1)
C(15)	−0.2289(4)	0.4769(3)	0.3973(3)	52.3(9)
C(16)	−0.0006(3)	0.2385(3)	0.3195(2)	42.2(8)
C(17)	−0.1135(3)	0.2424(2)	0.2415(2)	43.4(8)
C(18)	−0.0930(4)	0.2307(3)	0.1558(2)	53.1(9)
C(19)	−0.1970(4)	0.2314(3)	0.0827(3)	63(1)
C(20)	−0.3245(4)	0.2424(3)	0.0931(3)	66(1)
C(21)	−0.3472(4)	0.2510(3)	0.1771(3)	62(1)
C(22)	−0.2431(4)	0.2505(3)	0.2502(3)	51.6(9)
C(23)	0.1989(5)	0.3992(4)	0.2229(3)	68(1)
C(24)	0.2740(5)	0.3141(4)	0.2507(3)	64(1)
C(25)	0.3579(4)	0.3098(4)	0.3335(3)	67(1)
C(26)	0.3697(5)	0.3900(5)	0.3912(4)	76(1)
C(27)	0.2974(6)	0.4743(4)	0.3649(4)	80(2)
C(28)	0.2115(6)	0.4785(4)	0.2812(4)	79(2)

^a The anisotropic thermal parameters are given in the form of their isotropic equivalents (in 10³ Å²).

Table 4
Selected bond distances (Å) and angles (°) for **1b**

Ru–C(1)	2.033(3)		
Ru–C(2)	2.203(3)	C(1)–C(2)	1.426(4)
Ru–C(9)	2.194(3)	C(1)–C(9)	1.458(5)
Ru–C(16)	2.186(3)	C(1)–C(16)	1.432(4)
Ru–C(23)	2.223(4)	C(23)–C(24)	1.401(6)
Ru–C(24)	2.214(4)	C(24)–C(25)	1.372(6)
Ru–C(25)	2.208(4)	C(25)–C(26)	1.390(7)
Ru–C(26)	2.207(5)	C(26)–C(27)	1.374(7)
Ru–C(27)	2.208(5)	C(27)–C(28)	1.391(8)
Ru–C(28)	2.197(5)	C(23)–C(28)	1.386(7)
C(2)–C(1)–C(9)	110.7(3)	C(1)–C(2)–C(3)	127.7(3)
C(2)–C(1)–C(16)	115.0(3)	C(1)–C(9)–C(10)	128.6(3)
C(9)–C(1)–C(16)	118.0(3)	C(1)–C(16)–C(17)	127.8(3)

4. Crystal structures

The comparison between both crystal structures shows the effect that the isomerism has on the relative orientation of the molecules. It must be noted that the crystals of **1a** and **1b** contain the racemic mixtures of both possible enantiomers. Compound **1a** with the pro-

Table 5
Crystallographic and selected experimental data for **1a** and **1b**

Compound	1a	1b
Formula	C ₂₈ H ₂₄ Ru	C ₂₈ H ₂₄ Ru
Crystal shape	Prism	Prism
Crystal colour	Yellow	Yellow
Crystal size (mm)	0.16 × 0.20 × 0.64	0.16 × 0.24 × 0.56
Crystal system	Trigonal	Monoclinic
<i>M</i> (g mol ^{−1})	461.54	461.54
Space group	<i>P</i> 31 <i>c</i> (No. 159)	<i>P</i> 2 ₁ / <i>c</i> (No. 14)
Unit cell dimensions		
<i>a</i> (Å)	12.457(7)	10.330(2)
<i>b</i> (Å)	12.457(7)	13.526(4)
<i>c</i> (Å)	15.95(1)	15.402(3)
β (°)		103.05(3)
<i>Z</i>	12/3	4
ρ_{calc} (g cm ^{−3})	1.43	1.46
μ (Mo–K α) (cm ^{−1})	7.42	7.59
Empirical transmission	89.00–99.98	93.89–99.98
Factors		
<i>F</i> (000)	944.0	944.0
Scan range (°)	29	24
<i>T</i> (K)	293	293
Reflections measured	6260	3398
Indep. refl. obs.	2145	2379
[<i>I</i> ≥ 2 σ (<i>I</i>)]		
Final <i>R</i> indices <i>R</i> ₁ , <i>wR</i> ₂	0.0356, 0.0812	0.0253, 0.0537
[<i>I</i> ≥ 2 σ (<i>I</i>)]		
Final <i>R</i> indices <i>R</i> ₁ , <i>wR</i> ₂	0.0635, 0.1008	0.0382, 0.0620
All data		
Goodness-of-fit	1.125	1.087
Parameters refined	234	359
Residual density	1.246, −0.914	0.391, −0.270
Maximum, minimum $\Delta\rho$ (e Å ^{−3})		

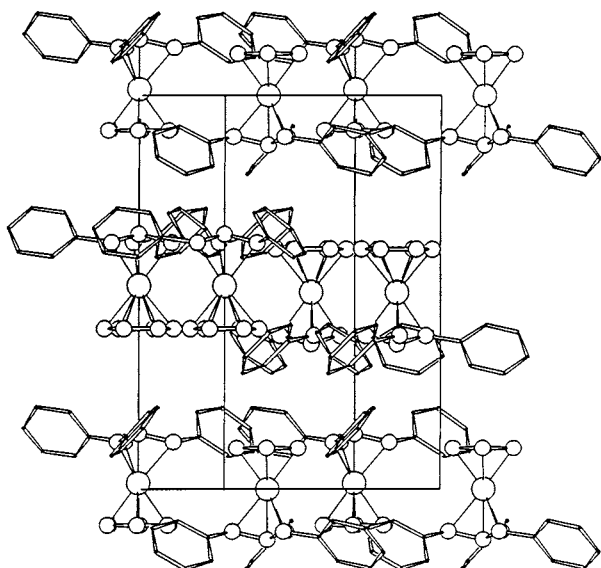


Fig. 3. Crystal packing of **1a**. SCHAKAL view perpendicular to the trigonal axis.

pellier-like ligand arrangement retains its threefold site-symmetry in the lattice. This compound crystallises in a layer structure (Fig. 3). In spite of the polar space group $P31c$, all molecules are arranged in an end-to-end fashion. The three-dimensional arrangement of the molecules will determine the macroscopic properties of the crystal. We have determined the unit cell parameters at different temperatures and the results show that the layer structure is manifested in the strong anisotropy of the thermal expansion (Fig. 4).

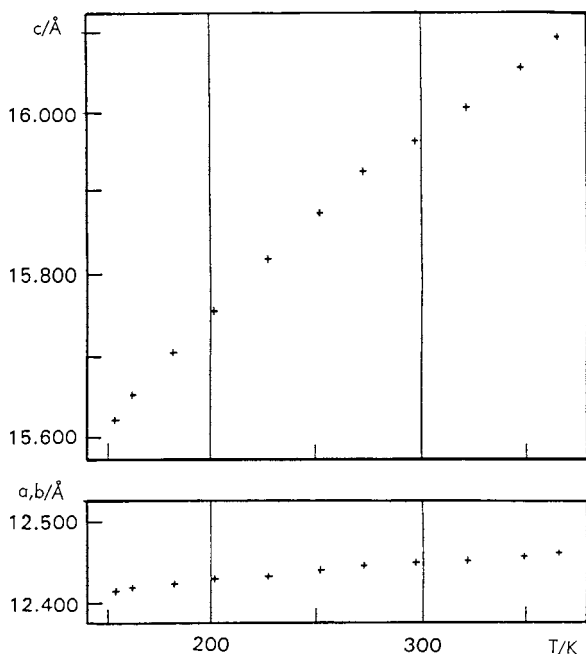


Fig. 4. Crystal lattice parameters of **1a** as a function of temperature.

Whereas both crystallographically independent molecules of **1a** have nearly identical molecular structures, their local environment in the crystal lattice is very different. This is expressed in the molecular coordination [11,12]. We determine the first-neighbouring molecules on the basis of intermolecular contacts. This way, we have found coordination numbers of 14 and 18 for the molecules on $(0\ 0\ z)$ and on $(2/3\ 1/3\ z)$ respectively. The different coordination is represented by projections along the C_3 -axis (Fig. 5(a) and (b)). For clarity, Fig. 5(c) shows the positions of the metal centres only. The geometry of the coordination polyhedron can be described as a hexagonal prism with a sixfold capping. The molecule with coordination number 14 (Fig. 5(a)) has contacts with two molecules on the threefold axis (above and below the original molecules).

After solving this structure, we found that a very similar arrangement in the solid state was reported for $[\text{Ta}(\text{TBM})(\eta^5\text{-C}_5\text{H}_5)(\text{CH}_3)_2]$ **3** [13]. This compound crystallises in the same space group $P31c$, which is very rare [13]. We also note that both compounds do crystallise with nearly identical positions for the metal atoms and for the carbon atoms of the TBM fragment. Compared to **3**, the atomic co-ordinates for **1a** show that our crystal adopts the opposite polarity. In the former case, the structural refinement revealed a substantial amount of inversion twinning (which is not found here). The peculiar structure of **3** was recognised and details were discussed [13]. In **3**, the imposed crystallographic C_3 symmetry causes the disorder between the CH_3 and the C_5H_5 groups in spite of their sterically very different demand. Similarities between the crystal packing of molecules can often be found in the molecular enclosure shell but this does not necessarily lead to crystallisation in the same space group [14].

The diastereoisomer **1b** shows a considerably different packing arrangement (Fig. 6). We observe a molecular co-ordination number of 11, Fig. 7 shows the molecular enclosure shell. Compared to **1a**, the lower symmetry of **1b** allows a more tight packing arrangement, because the phenyl ring ligands can interlock better with neighbouring molecules. This leads to a better match of the subunits in the crystal structure. This effect can be quantified by the values of the packing coefficient C_k , which are given as the ratio between the molecular and the crystal volumes [11]. Because an interpretation of these coefficients is useful on a relative basis, both diastereomeric isomers can be compared. Here, values of $C_k = 68.2\%$ for **1b** and 65.0% for **1a** were determined by the method of Gavezzotti [15]. In comparison, the TMM metal complex **2** is more tightly packed in the solid state (with a value for C_k of 71.0%), since this molecule has a rather ellipsoidal shape and no bulky substituents prevent close packing. The packing of **2** closely resembles that of free benzene, as shown in Fig. 8 (a) and (b). Such close relationships

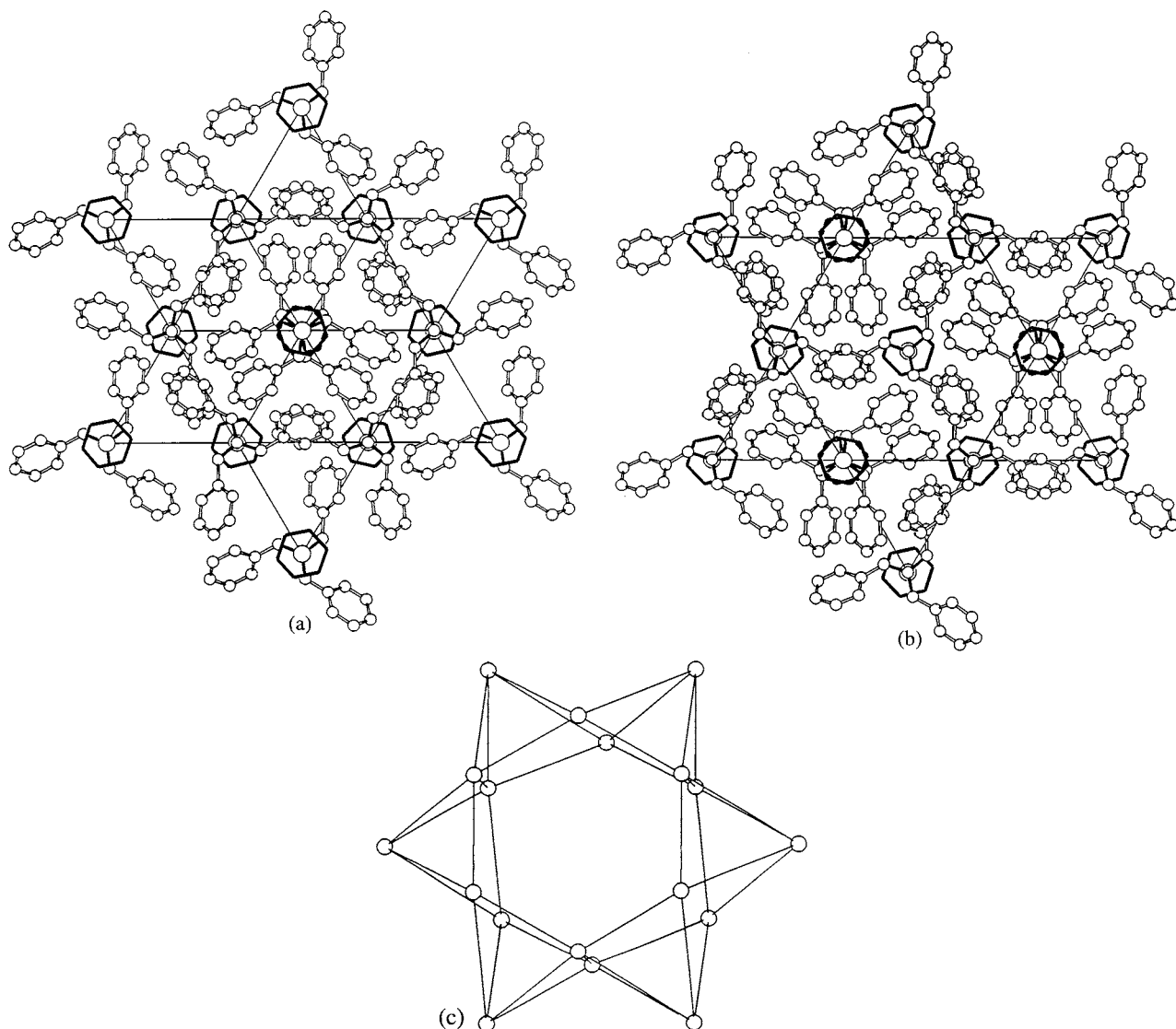


Fig. 5. (a) Crystal packing of **1a**. SCHAKAL view parallel to the trigonal axis, showing the coordination of the molecule on (0 0 z). (b) Crystal packing of **1a**. SCHAKAL view parallel to the trigonal axis, showing the coordination of the molecule on (2/3 1/3 z). (c) Same as (b), showing only the metal atom positions of the coordinating molecules. The view is slightly tilted from the trigonal axis.

between the crystalline packing of the metal complex and the free ligand have also been observed by Braga and are especially obvious in the molecular enclosure shell [16].

5. Conclusions and outlook

The reaction products **1a** and **1b** show that diastereoisomers may result when the dianion of TBM is treated with transition metal halogenides. The products will not necessarily contain only the C_3 -symmetrical propeller-like ligand.

The close analogy between the crystal structures of **1a** and **3** shows that it is the propeller-shaped ligand TBM which determines how these transition metal complexes are arranged in the crystal lattice. The

strongly directive effect of this fragment may be used to design other crystal structures with a similar layer arrangement. This fragment may be employed as a synthon in crystal engineering [17].

6. Experimental and calculations

6.1. Synthesis of the $(\eta^6\text{-Benzene})(\eta^4\text{-tribenzylidene-methane})$ ruthenium isomers **1a** and **1b**

Experiments were carried out in a dry, oxygen-free nitrogen atmosphere by means of conventional Schlenk techniques. Solvents were dried and distilled under nitrogen prior to use. Alumina for chromatography (Fa. Woelm, ICN-Adsorbentien) was heated in vacuo at 300°C and, after cooling, deactivated with deoxy-

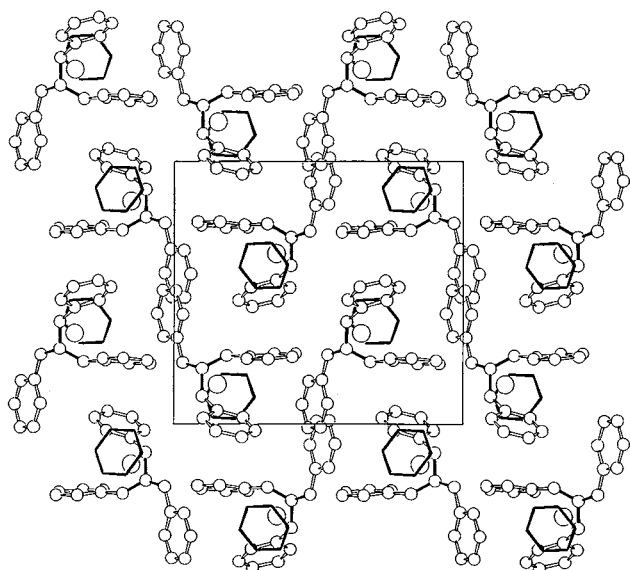


Fig. 6. SCHAKAL view of the crystal packing of **1b**.

generated water (7%). NMR spectra were recorded in CDCl_3 on a Bruker WP-80 PFT spectrometer (^1H : 80 MHz) and a Bruker WH-270 spectrometer (^{13}C : 67.88 MHz). The mass spectrum was recorded using a MAT CH 5-DF (Varian) spectrometer at 70 eV.

$[\text{RuCl}_2(\text{C}_6\text{H}_6)_2]$ [**18**] (1.81 g, 1.62 mmol) is added with stirring to $[\text{Li}(\text{TMEDA})_2][\text{C}(\text{CHPh})_3]$ [**2**] (1.76 g, 3.32 mmol) in THF (100 ml) at -78°C . Stirring is continued while the mixture was allowed to warm up to r.t. within 1 h. After removal of all volatiles in vacuo the residue was dissolved in toluene and the solution was filtered through a frit with alumina (200 ml). This process was repeated with toluene–hexane (1:1) as solvent. The solvent was again removed. The residue was

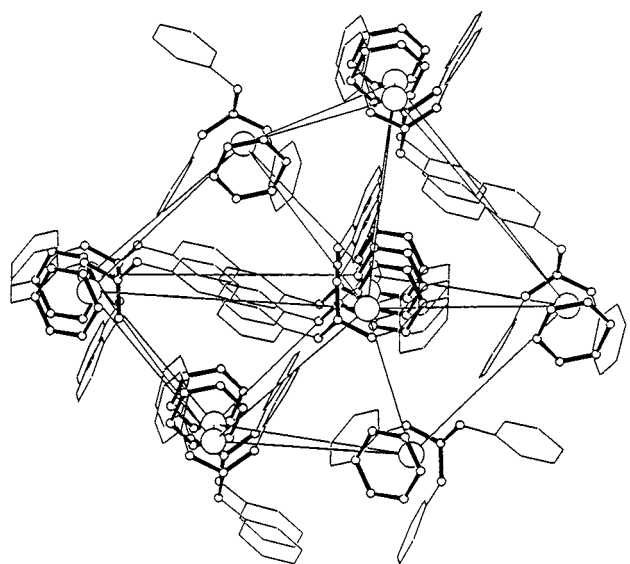
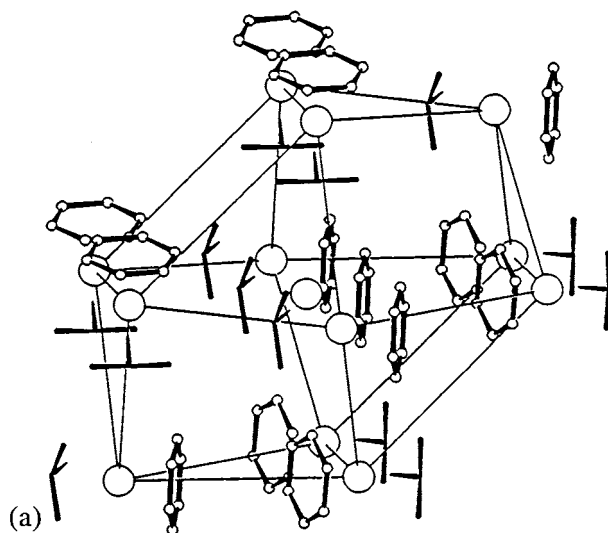
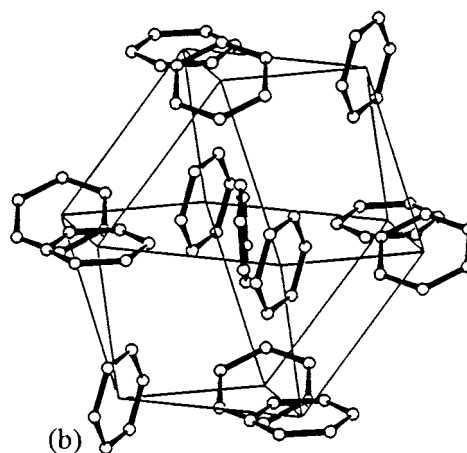


Fig. 7. SCHAKAL view showing the molecular co-ordination of **1b**.



(a)



(b)

Fig. 8. (a) SCHAKAL view showing the molecular co-ordination of **2**. (b) SCHAKAL view showing the molecular co-ordination of benzene (co-ordinates are from lit. [26]).

then stirred with hexane (200 ml) overnight. Filtration and cooling to -30°C gave **1a** (0.30 g, 20%) as a yellow crystalline powder; m.p. (dec.) $232\text{--}233^\circ\text{C}$. Found: C, 72.9; H, 5.3. $\text{C}_{28}\text{H}_{24}\text{Ru}$ Anal. Calc.: C, 72.9; H, 5.2%. The mother liquor was concentrated. Chromatography over alumina with hexane as eluent gave a light yellow band. Concentrating the yellow elute and cooling to -78°C gave **1b** (0.10 g, 7.0%) as yellow crystals; m.p. (dec.) $138\text{--}140^\circ\text{C} > 255^\circ\text{C}$.

1a: ^1H -NMR (ppm): 7.05–7.25 m (3 Ph), 5.13 s (C_6H_6), 4.18 s (3 CHPh). ^{13}C -NMR (ppm), J (Hz): 143.6 s (C_i), 129.4 d (158, C_m), 127.5 d (158, C_o), 124.2 d (161, C_p); 95.6 s (CC_3), 82.5 d (172, C_6H_6), 61.2 d (156, 3 CHPh). MS (m/z , I_{rel} (%)): 461 (83; $[\text{M}^+]$), 383 (100; $[\text{M}^+] - \text{C}_6\text{H}_6$).

1b: ^1H -NMR (ppm) 7.0–7.2 m (Ph), 6.7 m (2 Ph), 5.35 s (C_6H_6), 4.41 d and 3.32 d ($^4J = 1.5$ Hz, CHPh), 3.15 s (CHPh); for assignment see text. ^{13}C -NMR (ppm), J (Hz): 143.2 s, 142.6 s and 141.6 s (C_i), 132.0

m, 131.0 m, 130.1 m, 127.6 m, 126.5 m and 126.5 m (C_o and C_m), 124.6 m, 124.4 m and 124.2 m (C_p); 96.4 s (CC_3), 83.0 d (173, C_6H_6), 67.6 d (147, $CHPh$), 67.1 d (149, $CHPh$), 59.7 d (158, $CHPh$).

6.2. Determination of the structures of **1a** and **1b**

Data sets were obtained using an Enraf–Nonius CAD4 diffractometer (ω -scan mode, monochromatic Mo– K_α radiation, $\lambda = 0.7093 \text{ \AA}$). The reflections were corrected for Lp effects using the program MoLEN [19] and for absorption using ψ -scans [20]. Both structures were solved by Patterson and Fourier methods. For better comparison with the structure of **3**, the co-ordinates of **1a** (Table 1) were transformed into the same asymmetric unit. The refinement was carried out using the program SHELXL93 based on F^2 [21]. Anisotropic thermal parameters were refined for all non hydrogen atoms. With the exception of two hydrogen atoms H9 and H10 in **1a**, which were incorporated into calculated positions, all hydrogen atoms were located and refined with isotropic thermal parameters. For **1a**, the polarity could be determined unambiguously from the absolute structure parameter of 0.06(7) [22]. Results are given in Tables 1–5. Graphical representations of the results were carried out using the programs ORTEP-III [23] and SCHAKAL [24]. The unit cell parameters shown in Fig. 4 were determined on a CAD4 diffractometer with Cu– K_α radiation and 25 centred reflections in the range of ($26 < \theta < 30^\circ$). Crystallographic data for the structural analysis have been deposited with the Cambridge Crystallographic Data Centre, CCDC-116616 for **1a** and CCDC-116617 for **1b**. Copies of this information may be obtained free of charge from the Director, CCDC, 12 Union Rd, Cambridge CB2 1EZ, UK (Fax: +44-1223-336-033; e-mail: deposit@ccdc.cam.ac.uk; or <http://www.ccdc.cam.ac.uk>).

6.3. Coordination numbers

To find out which molecules are forming the enclosure shell, we calculated the distances between all atoms within a reference molecule to all remaining atoms which lie within three unit cells in each direction. If a molecule contains at least one atom which shows a contact to the reference molecule, we consider it as being a part of the enclosure shell. As a cut-off distance, we are using the sum of the van der Waals radii multiplied by 1.2. For these, we are using the values as in Lit. [15] and of 2.10 \AA for Ru. Calculations were carried out with the program BUILD [25], which uses the atomic coordinates and the crystallographic symmetry operations.

6.4. Packing coefficients

Packing coefficients were calculated by the numerical method of A. Gavezzotti by calculating the molecular

volume V_m [15]. Here, we are counting the number of points that fall inside at least one sphere describing an atom (using the van der Waals radius). The point mesh was refined until convergence was reached.

Acknowledgements

The authors are indebted to Dr U. Englert for helpful discussions. Generous support of this work by the Fonds der Chemischen Industrie is gratefully acknowledged.

References

- [1] M.D. Jones, R.D.W. Kemmitt, *Adv. Organomet. Chem.* 27 (1987) 279.
- [2] R.S. Lokey, N.S. Mills, A.L. Rheingold, *Organometallics* 8 (1989) 1803.
- [3] G.E. Herberich, U. Englert, L. Wesemann, P. Hofmann, *Angew. Chem.* 103 (1991) 329; *Angew. Chem. Int. Ed. Engl.* 30 (1991) 313.
- [4] G.E. Herberich, T.P. Spaniol, *J. Chem. Soc. Chem. Commun.* (1991) 1457; *J. Chem. Soc. Dalton Trans.* (1993) 2471.
- [5] G.C. Bazan, G. Rodriguez, B.P. Cleary, *J. Am. Chem. Soc.* 116 (1994) 2177.
- [6] D. Wilhelm, T. Clark, R.v.R. Schleyer, K. Buckl, G. Boche, *Chem. Ber.* 116 (1983) 1669.
- [7] D. Wilhelm, H. Dietrich, T. Clark, W. Mahdi, A.J. Kos, P.v.R. Schleyer, *J. Am. Chem. Soc.* 106 (1984) 7279.
- [8] G. Rodriguez, G.C. Bazan, *J. Am. Chem. Soc.* 117 (1995) 10155.
- [9] G. Rodriguez, G.C. Bazan, *J. Am. Chem. Soc.* 119 (1997) 343.
- [10] K. Ehrlich, G.F. Emerson, *J. Am. Chem. Soc.* 94 (1972) 2464.
- [11] A.I. Kitaigorodsky, *Organic Chemical Crystallography*, Consultants Bureau, New York, 1961.
- [12] A.I. Kitaigorodsky, *Molecular Crystals and Molecules*, Academic Press, New York, 1973.
- [13] W.P. Schaefer, R.E. Marsh, G. Rodriguez, G.C. Bazan, *Acta Crystallogr. B52* (1996) 465.
- [14] D. Braga, F. Grepioni, P. Sabatino, *J. Chem. Soc., Dalton Trans.* (1990) 3137.
- [15] A. Gavezzotti, *J. Am. Chem. Soc.* 105 (1983) 5220.
- [16] D. Braga, F. Grepioni, *Organometallics* 10 (1991) 2563.
- [17] G.R. Desiraju, *Angew. Chem.* 107 (1995) 2541; *Angew. Chem. Int. Ed. Engl.* 34 (1995) 2328.
- [18] M.A. Bennett, A.K. Smith, *J. Chem. Soc. Dalton Trans.* (1974) 233.
- [19] C.K. Fair, *MoLEN, An Interactive Structure Solution Procedure*, Enraf Nonius, Delft, The Netherlands, 1990.
- [20] A.C.T. North, D.C. Phillips, F. Scott Mathews, *Acta Crystallogr. A24* (1968) 351.
- [21] G.M. Sheldrick, SHELXL93, A Program for Crystal Structure Refinement, University of Göttingen, Göttingen, Germany (1993).
- [22] H.D. Flack, *Acta Crystallogr. A39* (1983) 876.
- [23] C.K. Johnson, M.N. Burnett, ORTEP-III, Oak Ridge Thermal Ellipsoid Program for Crystal Structure Illustrations, Oak Ridge National Laboratory, Oak Ridge, TN, USA, 1996.
- [24] E. Keller, SCHAKAL88-a FORTRAN program for the graphic representation of molecular and crystallographic models, Freiburg (1988).
- [25] U. Englert, FORTRAN program BUILD, RWTH Aachen, Germany (1992).
- [26] G.E. Bacon, N.A. Curry, S.A. Wilson, *Proc. Roy. Soc. A* 279 (1964) 98.